International Scholarly Research Network
ISRN Nanotechnology
Volume 2011, Article ID 893879, 3 pages
doi:10.5402/2011/893879

Research Article

Microwave-Assisted Synthesis Core-Fe_3O_4 Shell-Au Cubic Nanoparticles

Manuel Ramos,[1,2] Karina Castillo,[1] Domingo A. Ferrer,[3] Rurik J. Farias,[2] Sergio Flores,[2] and Russell R. Chianelli[1]

[1] *Materials Research and Technology Institute, UT-El Paso, El Paso, TX 79968, USA*
[2] *Departamento de Física y Matemáticas, Universidad Autónoma de Ciudad Juárez, Ciudad Juárez, MX 32300, USA*
[3] *Microelectronics Research Center, UT-Austin, Austin, TX 78751, USA*

Correspondence should be addressed to Manuel Ramos, manuel.ramos@uacj.mx

Received 18 July 2011; Accepted 17 August 2011

Academic Editors: I.-C. Chen and J. Das

Core-Shell (Fe_3O_4/Au) nanoparticles were synthesized using iron II chloride tetrahydrate ($FeCl_2H_2O$) and potassium tetrachloroaurate III ($AuCl_4K$) precursors under microwave-assisted conditions. Products were analyzed using field emission gun electron microscope in transmission and scanning modes; energy disperse X-ray spectroscopy performed during STEM measurements indicated a signal for gold *K* and *M* signals at 9 keV and 13 keV, respectively, confirming Au atoms at nanoparticle's perimeter and Fe-*L* signal at 8 keV to be at the center.

1. Introduction

Chemical synthesis, fabrication, and applications of nanoparticles have been an evolving topic in the material science of advanced materials; this is attributed mainly to their specific electronic properties, which in many cases differ from as when they are present in bulk, making them strong chemical entities as antibacterial [1], solid-state electronics [2], catalytic reactions [3], optical physics, and petroleum research [4]. In particular, magnetic nanoparticles have attracted a special interest for two main reasons: (1) implementation as contrast agents for magnetic resonance imaging (MRI) [5], (2) magnetic material for data storage in solid-state electronics (SSE) [6]. The achievement of standardized shape and high-quality nanoparticles properties will depend solely on synthesis-fabrication method which is dependable on appropriate precursor solutions ratios and in some occasions a reductant agent [7–11]. Optical properties can be tuned by controlling the coating thickness; previous studies indicate the possibility to tune surface plasmonic properties of Fe_3O_4/Au/Ag from $\lambda = 560$ nm (red shift) to $\lambda = 501$ nm (blue shift) with the addition of nonmagnetic layers (Au or Ag); however, it will reduce magnetic strength of (Fe_3O_4) nanoparticles [12]. Other authors achieved spindle-shaped hematite (Fe_2O_3) using a hydrothermal method of synthesis, and particle shapes depend only on 3-aminopropyl trimethoxysilane (APTMS) which acted as a reduction agent in generating amine moiety-coated surface [13, 14]. This paper presents a microwave-assisted synthesis of cubic core-shell Fe_3O_4/Au nanoparticles along with atom-resolved scanning transmission electron microscopy and energy disperse X-ray spectroscopy profiles.

2. Synthesis of AuFe_3O_4Cubic Nanoparticles

To avoid any contaminant variations on the results, before any chemical reaction, all glassware was cleaned using aqua regia in a concentration ratio of $HCl/HNO_3 = 3:1$. The synthesis consisted of two main steps. (1) Synthesis of Fe_3O_4 by using iron II chloride tetrahydrate ($FeCl_2 \cdot H2O$ Alfa Aesar) by dissolving 70 mg in distilled water and slowly titrated for 4 h with 40 mL of 5 M NaOH solution to form iron II hydroxide ($Fe(OH)_2$). The iron II hydroxide solution was oxidized to form Fe_3O_4 using microwave-assisted synthesis (Multiwave 2000) at a constant temperature of 120°C for 30

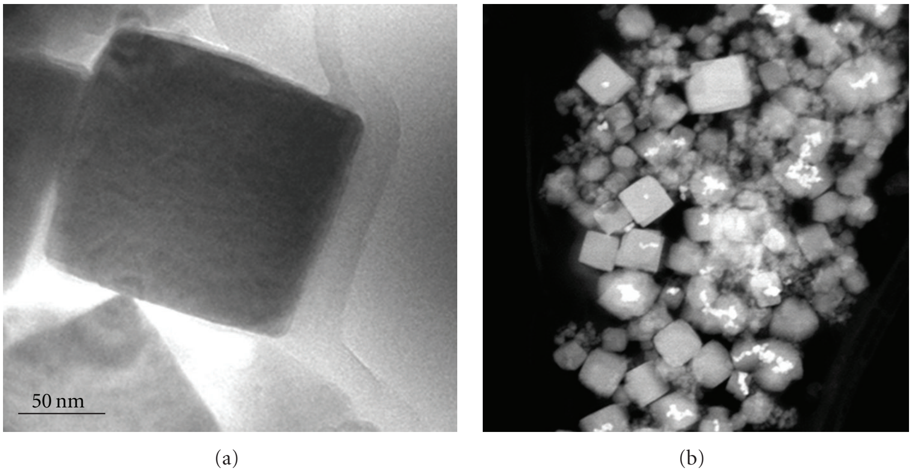

Figure 1: (a) HRTEM image of Fe_3O_4/Au nanoparticles at scale of 100 nm confirming cubic shape and (b) STEM image indicate that the majority of Fe_3O_4/Au nanoparticles have cubic shape.

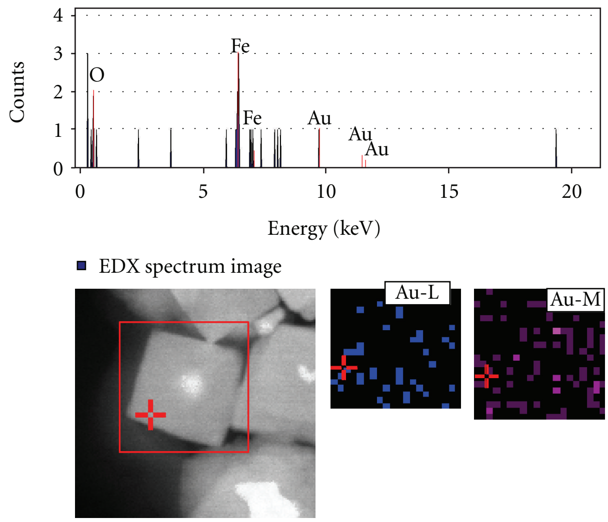

Figure 2: Energy disperse X-ray profile and STEM image indicating L and M signals at perimeter (red cross) corresponding to gold.

minutes; products were washed and centrifuged to remove any sodium chloride (NaCl) residue and then set to dry in an open-flow furnace at 100°C for 10 min.

(2) There is a second solution, where Fe_3O_4 and potassium tetrachloroaurate (III) in distilled water were dissolved to create gold shell onto Fe_3O_4 nanoparticles. This second reaction will reduce gold from Au^{+3} to Au^0 sodium citrate tribasic dehydrate. To quench the reaction, large amounts of distilled water were applied, followed by filtration of products and drying in open-flow furnace at 80°C for 30 min.

The stoichiometry of both reactions is as follows:

(1) $FeCl_2 \cdot H_2O + 2NaOH \longrightarrow Fe(OH)_2 + 2NaCl + H_2O$

(2) $Fe_3O_4 + KAuCl_4 + Na_3C_6H_5O_7 \longrightarrow AuFe_3O_4 + NaC_6H_5O_7 + KCl + 2NaCl + Cl_2$

3. Results and Discussion

3.1. Scanning Transmission Electron and Energy Disperse X-ray. Morphology of products ($AuFe_3O_4$) was studied by high-resolution transmission electron microscopy using an FEI Tecnai TF20 equipped with an STEM unit, high-angle annular dark-field (HAADF) detector, and X-Twin lenses. Just one drop of $AuFe_3O_4$/isopropanol solution was placed into a lacey/carbon (EMS LC225-Cu) grid. The operational voltage was kept constant at 200 kV in both dark field (DF) and bright field (BF) mode images. Scherzer defocus condition was set at $\Delta f_{\text{Sch}} = -1.2(C_s\lambda)^{1/2}$. Energy disperse X-ray analysis (EDX) was performed using a solid angle of 0.13 sr in the detector. Cubic structure is observed by HRTEM as presented in **Figure** 1; in order to locate the gold on nanoparticles surface, a profile was created using EDX while performing STEM as presented in Figures 2 and 3;

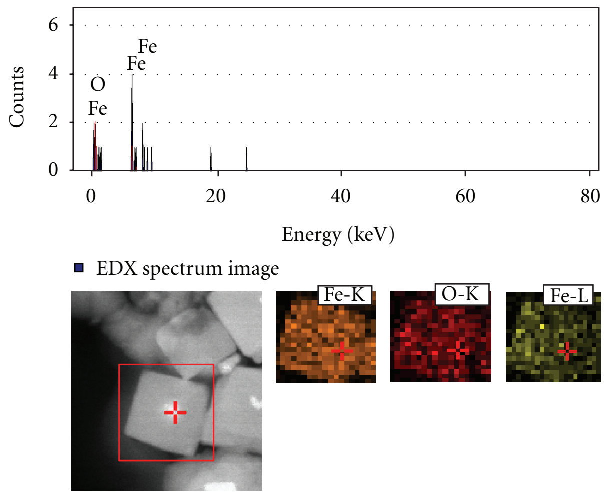

Figure 3: Energy disperse X-ray showing K and L signals corresponding to Fe when probe is at center and STEM image.

clearly K and M signals at 9 to 13 keV indicate the presence of gold at perimeter, while Fe-L signal at 8 keV appears when probing nanoparticle center.

4. Conclusions

A successful synthesis of cubic-shaped core-shell Fe_3O_4/Au nanoparticles was achieved using microwave-assisted synthesis. STEM and HRTEM confirm cubic shape. Energy disperse X-ray analysis profiles indicate peak intensities from 9 to 13 keV for gold at the perimeter and 8 keV for iron at the center also confirming a core-shell array.

Acknowledgment

The authors thank The National Nanotechnology Infrastructure Network (NNIN) Research Program of the Microelectronic Research Center of UT-Austin, the Consejo Nacional de Ciencia y Tecnología, México for their economic support, and the Materials Research and Technology Institute of UT-El Paso.

References

[1] L. Liu, K. Xu, H. Wang et al., "Self-assembled cationic peptide nanoparticles as an efficient antimicrobial agent," *Nature Nanotechnology*, vol. 4, no. 7, pp. 457–463, 2009.

[2] D. Ghosh and S. Chen, "Solid-state electronic conductivity of ruthenium nanoparticles passivated by metal-carbon covalent bonds," *Chemical Physics Letters*, vol. 465, no. 1–3, pp. 115–119, 2008.

[3] Y. Mei, G. Sharma, Y. Lu et al., "High catalytic activity of platinum nanoparticles immobilized on spherical polyelectrolyte brushes," *Langmuir*, vol. 21, no. 26, pp. 12229–12234, 2005.

[4] T. Otake, D. J. Wesolowski, L. M. Anovitz, L. F. Allard, and H. Ohmoto, "Experimental evidence for non-redox transformations between magnetite and hematite under H2-rich hydrothermal conditions," *Earth and Planetary Science Letters*, vol. 257, no. 1-2, pp. 60–70, 2007.

[5] M. V. Yigit, L. Zhu, M. A. Ifediba et al., "Noninvasive MRI-SERS imaging in living mice using an innately bimodal nanomaterial," *ACS Nano*, vol. 5, no. 2, pp. 1056–1066, 2011.

[6] T. Hyeon, "Chemical synthesis of magnetic nanoparticles," *Chemical Communications*, vol. 9, no. 8, pp. 927–934, 2003.

[7] D. Ferrer, A. Torres-Castro, X. Gao, S. Sepúlveda-Guzmán, U. Ortiz-Méndez, and M. José-Yacamán, "Three-layer core/shell structure in Au-Pd bimetallic nanoparticles," *Nano Letters*, vol. 7, no. 6, pp. 1701–1705, 2007.

[8] R. Nagarajan et al., *Nanoparticles: Synthesis, Stabilization, Passivation, and Functionalization*, ACS Symposium Series, Washington, DC, USA, 2008.

[9] M. Spuch-Calvar, J. Pérez-Juste, and L. M. Liz-Marzán, "Hematite spindles with optical functionalities: growth of gold nanoshells and assembly of gold nanorods," *Journal of Colloid and Interface Science*, vol. 310, no. 1, pp. 297–301, 2007.

[10] Y. Zhang, E. W. Shi, Z. Z. Chen, and B. Xiao, "Fabrication of ZnO hollow nanospheres and "jingle bell" shaped nanospheres," *Materials Letters*, vol. 62, no. 8-9, pp. 1435–1437, 2008.

[11] Y. Sun, B. T. Mayers, and Y. Xia, "Template-engaged replacement reaction: a one-step approach to the large-scale synthesis of metal nanostructures with hollow interiors," *Nano Letters*, vol. 2, no. 5, pp. 481–485, 2002.

[12] Z. Xu, Y. Hou, and S. Sun, "Magnetic core/shell Fe_3O_4/Au and Fe_3O_4/Au/Ag nanoparticles with tunable plasmonic properties," *Journal of the ACS*, vol. 129, no. 28, pp. 8698–8699, 2007.

[13] J. Lin, W. Zhou, A. Kumbhar et al., "Gold-coated iron (Fe@Au) nanoparticles: synthesis, characterization, and magnetic field-induced self-assembly," *Journal of Solid State Chemistry*, vol. 159, no. 1, pp. 26–31, 2001.

[14] Z. Ma, H. Han, S. Tu, and J. Xue, "Fabrication of shape-controlled hematite particles and growth of gold nanoshells," *Colloids and Surfaces A: Physicochemical and Engineering Aspects*, vol. 334, no. 1–3, pp. 142–146, 2009.